Desiana Vidayanti

SINERGI Stress-Strain Petobo - DV(22112025) IEEE

Universitas Islam Negeri Raden Fatah - no repository 26

Document Details

Submission ID
trn:oid:::3618:122332754

Submission Date
Nov 22, 2025, 5:31 PM GMT+7

Download Date
Nov 22, 2025, 5:38 PM GMT+7

File Name
SINERGI Stress-Strain Petobo - DV(22112025) IEEE.pdf

File Size
957.6 KB

13 Pages

6,819 Words

38,477 Characters

16% Overall Similarity

The combined total of all matches, including overlapping sources, for each database.

Filtered from the Report

- Bibliography
- Quoted Text
- Small Matches (less than 8 words)

Match Groups

74 Not Cited or Quoted 15%
Matches with neither in-text citation nor quotation marks

5 Missing Quotations 1%
Matches that are still very similar to source material

0 Missing Citation 0%
Matches that have quotation marks, but no in-text citation

0 Cited and Quoted 0%
Matches with in-text citation present, but no quotation marks

Top Sources

10% Internet sources
8% Publications
12% Submitted works (Student Papers)

Match Groups

- **74** Not Cited or Quoted 15%
  Matches with neither in-text citation nor quotation marks
- **5** Missing Quotations 1%
  Matches that are still very similar to source material
- **0** Missing Citation 0%
  Matches that have quotation marks, but no in-text citation
- **0** Cited and Quoted 0%
  Matches with in-text citation present, but no quotation marks

Top Sources

10% Internet sources
8% Publications
12% Submitted works (Student Papers)

Top Sources

The sources with the highest number of matches within the submission. Overlapping sources will not be displayed.

1	Student papers	
Trisakti University on 2025-09-19		2%
2	Internet	
publikasi.mercubuana.ac.id		<1%
3	Internet	
repository.unsri.ac.id		<1%
4	Student papers	
Universitas Diponegoro on 2022-03-29		<1%
5	Publication	
Emma Gardiner, Mark Stringer, Misko Cubrinovski, Sean Rees, Chris McGann. "Eff...		<1%
6	Student papers	
The Hong Kong Polytechnic University on 2009-06-22		<1%
7	Student papers	
University Tun Hussein Onn Malaysia on 2025-02-22		<1%
8	Internet	
hdl.handle.net		<1%
9	Publication	
Jiarui Chen, Yaolan Tang, Jianhong Ye, Chunshun Zhang, Zhenghong Lin, Congyin...		<1%
10	Publication	
Shaurya Sood, Gabriele Chiaro, Thomas Wilson, Mark Stringer. "Monotonic Drain...		<1%

11	Publication	
Yang Xiao, Shuang Liu, Qingyun Fang, Ninghao Wang, Hanlong Liu. "Thermo-mec...		<1%
12	Student papers	
Curtin University of Technology on 2017-11-03		<1%
13	Publication	
Md. Zillal Hossain, Md. Zoynul Abedin, Md. Rejwanur Rahman, Md. Nafiul Haque, ...		<1%
14	Publication	
Xiao Xie, Yumin Chen, Saeed Sarajpoor, Yutang Chen, Yi Han. "Influence of plastic...		<1%
15	Internet	
jurnal.pnj.ac.id		<1%
16	Internet	
hub.hku.hk		<1%
17	Internet	
mafiadoc.com		<1%
18	Publication	
Ilaria Farina, Giuseppe Lanzo. "Chapter 11 Energy-Based Method and Seismic Liq...		<1%
19	Student papers	
Imperial College of Science, Technology and Medicine on 2021-08-27		<1%
20	Publication	
Jerry A. Yamamuro, Poul V. Lade. "Steady-State Concepts and Static Liquefaction ...		<1%
21	Student papers	
Middle East Technical University on 2011-10-05		<1%
22	Student papers	
New Jersey Institute of Technology on 2021-11-07		<1%
23	Student papers	
University of Hong Kong on 2025-07-30		<1%
24	Internet	
ro.uow.edu.au		<1%

25 Internet

scholarworks.uark.edu <1%

26 Publication

HONG-JIAN LIAO, LI-JUN SU, WU-CHUAN PU, JIAN-HUA YIN. "Test and Numerical A... <1%

27 Publication

Nazile Ural, Zeki Gunduz. "Behavior of Nonplastic Silty Soils under Cyclic Loading"... <1%

28 Student papers

Ohio University on 2006-02-27 <1%

29 Student papers

University of Hong Kong on 2023-11-13 <1%

30 Student papers

University of Pretoria on 2016-09-13 <1%

31 Internet

research-repository.griffith.edu.au <1%

32 Internet

www.e3s-conferences.org <1%

33 Internet

www.mdpi.com <1%

34 Publication

Azeiteiro, Ricardo José Novo. "Numerical Simulation of Liquefaction-Related Phen... <1%

35 Publication

Charles W. W. Ng, W. T. Fung, C. Y. Cheuk, Liming Zhang. "Influence of Stress Rati... <1%

36 Publication

Constitutive Modelling of Granular Materials, 2000. <1%

37 Publication

Kangle Zuo, Xiaoqiang Gu, Jiachen Zhang, Rui Wang. "Exploring packing density, c... <1%

38 Student papers

Librarian NITT on 2025-11-21 <1%

39 Publication
Rodrigo Zorzal Velten, Nilo Cesar Consoli, Hugo Carlos Scheuermann Filho, Alexia ... <1%

40 Publication
S L Yang, R Sandven, L Grande. "Steady-state lines of sand–silt mixtures", Canadia... <1%

41 Publication
S. Leroueil. "Construction pore pressures in clay foundations under embankment... <1%

42 Publication
Sunil, B.M.. "Shear strength characteristics and chemical characteristics of leac... <1%

43 Student papers
University of South Australia on 2021-11-12 <1%

44 Publication
Yildirim, Sefa. "Numerical and Experimental Analysis of Single Pile Foundation Be... <1%

45 Publication
Zhehao Zhu. "Influence of Fine Particles on the Liquefaction Properties of a Refer... <1%

46 Internet
link.springer.com <1%

47 Internet
www.collectionscanada.ca <1%

48 Internet
www4.hcmut.edu.vn <1%

49 Publication
A Jalil, T F Fathani, I Satyarno, W Wilopo. "Nonlinear site response analysis approa... <1%

50 Student papers
Asian Institute of Technology on 2010-05-12 <1%

51 Publication
H. Than Trong Tran, H. Wong, Ph. Dubujet, T. Doanh. "Simulating the effects of in... <1%

52 Student papers
Indian Institute of Science, Bangalore on 2022-10-10 <1%

53 Student papers
Institute of Graduate Studies, UiTM on 2012-06-11 <1%

54 Publication
Jean-Jacques Fry, Norihisa Matsumoto. "Validation of Dynamic Analyses of Dams ... <1%

55 Publication
Jin Yuan, Rui Zhu, Yanpian Mao, Lanlan Xu, Jianfan Zhao, Chao Zhang, Shu Zhang. ... <1%

56 Publication
Mir Zeeshan Ali, Majid Hussain. "Impact of Particle Characteristics on the Static Li... <1%

57 Publication
Radhavi A. Samarakoon, Isaac L. Kreitzer, John S. McCartney. "Impact of initial eff... <1%

58 Student papers
Rowan University on 2025-06-09 <1%

59 Publication
Springer Series in Geomechanics and Geoengineering, 2008. <1%

60 Student papers
University of Dundee on 2025-05-18 <1%

61 Student papers
University of Edinburgh on 2022-03-31 <1%

62 Student papers
University of Newcastle on 2010-11-04 <1%

63 Student papers
University of South Australia on 2021-08-13 <1%

64 Student papers
University of South Australia on 2025-11-14 <1%

65 Publication
Yuyan Chen, Ali Khosravi, Alejandro Martinez, Jason DeJong. "Modeling the self-p... <1%

66 Internet
doaj.org <1%

67 Internet

mdpi-res.com <1%

68 Internet

ruor.uottawa.ca <1%

69 Internet

www.hallcounty.org <1%

70 Internet

www.ideals.illinois.edu <1%

71 Internet

www.researchgate.net <1%

SINERGI Vol. xx, No. x, February 20xx: xxx-xxx
http://publikasi.mercubuana.ac.id/index.php/sinergi
http://doi.org/10.22441/sinergi.xxxx.x.xxx

Stress-Strain Behavior and Residual Strength of Petobo Sand with Variable Fines Content after the 2018 Palu Liquefaction

Desiana Vidayanti[1,2], Paulus Pramono Rahardjo[1], Ramli Nazir[1]
[1]Department of Civil Engineering, Parahyangan Catholic University, Bandung, Indonesia
[2]Department of Civil Engineering, Mercu Buana University, Jakarta, Indonesia

Abstract
Liquefaction was one of the main causes of severe ground deformation during the 2018 Palu earthquake, particularly in the Petobo area where large-scale flow liquefaction occurred. Despite extensive field investigations, no laboratory-based residual shear strength data for Petobo soil have been available to explain the exceptional mobility of the flowslide. This study investigates the stress–strain response and residual strength of Petobo silty sand containing different proportions of fines through monotonic Consolidated Undrained (CU) triaxial tests. Reconstituted specimens were prepared using the moist tamping method with fines contents of approximately 9% and 26.4%, and tested under three levels of initial mean effective stress.The higher-fines specimen generated excess pore water pressure more rapidly and showed stronger contractive behavior at small strains. However, at larger strains, the 26.4% fines specimen mobilized greater residual strength, expressed as the ratio of residual deviator stress to initial mean effective stress (0.79-0.94), compared with the 9% fines specimen (0.85-0.89). These results indicate that fines increase contractive tendency during initiation but enhance resistance against large post-liquefaction deformation. The influence of fines on post-liquefaction behavior is therefore nonlinear and dependent on deformation stage and initial density. This study provides the first laboratory-based residual strength data of Petobo silty sand within the Critical State Soil Mechanics framework, clarifying its post-liquefaction resistance characteristics. The findings improve understanding of flow behavior in silty sands, offer mechanistic insight into the 2018 Petobo failure, and supply essential parameters for calibrating constitutive models and supporting liquefaction hazard mitigation in similar alluvial deposits in Central Sulawesi.

Keywords:
Contractive behavior; Critical state; Flow liquefaction; Silty sand; Undrained triaxial test

Article History:
Received: May 2, 2019
Revised: May 29, 2019
Accepted: June 2, 2019
Published: June 2, 2019

Corresponding Author:
Desiana Vidayanti, Department of Civil Engineering, Parahyangan Catholic University, Bandung, Indonesia.
Department of Civil Engineering, Universitas Mercu Buana, Jakarta, Indonesia
Email: desianavidayanti@gmail.com

INTRODUCTION

Liquefaction is one of the primary causes of severe infrastructure damage during major earthquakes. During the 2018 Palu earthquake, the Petobo area experienced one of the most destructive cases of flow liquefaction ever recorded worldwide, resulting in large-scale ground displacement and the devastation of residential areas and public facilities [1]–[4]. The event involved complex subsurface mechanisms, including confined aquifers, stratified layers, and undissipated pore-pressure migration [5]–[7], emphasizing the need for detailed laboratory investigation of the affected soils.

Although the Petobo flowslide has been widely studied from the perspectives of geomorphology, groundwater rise, hydrological triggering, and stratigraphic controls [5], [6] [7] no previous study has measured the post-liquefaction residual shear strength of Petobo soil. This parameter directly governs the distance that the liquefied mass can travel. As a result, a key mechanical input required to explain how the Petobo deposit moved hundreds of meters remains unknown. The absence of such data limits the accuracy of back-analyses and the ability to predict similar failures in the Palu region.

In general, loose saturated sand is highly susceptible to liquefaction due to its strongly contractive behavior, rapid pore-pressure buildup, and reduction of effective stress leading to loss of shear strength (Cetin & Bilge, 2022) [9], [10]. The presence of fine particles (fines) adds further complexity. At low contents, non-plastic fines can accelerate pore-pressure generation and reduce liquefaction resistance [11] [12], whereas at higher levels they may increase mixture density and improve resistance [11], [13], [14]. Plastic fines tend to reduce resistance more significantly [15]–[17]. Other factors, such as confining stress, particle morphology, and soil fabric, also influence the undrained response of silty sand [18][19]

Globally, most liquefaction research has focused on cyclic loading, which is relevant to the triggering process during earthquakes [20], [21]. However, the post-liquefaction residual shear strength which governs whether deformation will cease or evolve into catastrophic flow failure is more appropriately evaluated using monotonic undrained loading, as applied in the present study [22][23]. Incorporating both cyclic and monotonic perspectives is essential for understanding the mechanisms underlying the Palu event.

The Critical State Soil Mechanics (CSSM) framework provides an appropriate basis for analyzing liquefiable soils, particularly when effective stress approaches zero. The Critical State Line (CSL) defines the boundary shear strength at large strain, and numerous studies have confirmed the relevance of CSSM for evaluating the influence of fines and post-liquefaction behavior [24]–[26]. Experimental research on Palu soils has shown that fines content affects steady-state resistance (Artati et al., 2023), yet the stress–strain evolution and residual strength of Petobo silty sand up to the critical state have never been measured.

Residual shear strength is a key parameter determining whether a liquefied deposit will regain stability or transform into a catastrophic flow failure. It depends on fines content, relative density, and stress conditions, and several studies have reported low residual strength in silty sands at large strains [12], [27], [28]. Although field investigations of the 2018 Palu flowslide have provided valuable insights into stratigraphy and groundwater pathways [29], [30] no laboratory measurements of the residual shear strength of Petobo soil are currently available. Previous reconstructions relied on assumed residual strength values rather than direct measurements, creating a critical research gap for accurate hazard assessment.

Accordingly, the primary research question of this study is: To what extent does fines content influence the normalized residual shear strength ratio of very loose Petobo silty sand, and how does this behavior help explain the mobility observed during the 2018 flowslide?

The monotonic Consolidated Undrained (CU) triaxial test provides controlled measurement of contractive tendencies, pore-pressure generation, effective stress paths, and steady-state strength, making it well suited for evaluating post-liquefaction behavior and addressing this research gap [22][23]

Based on this background, this study evaluates the stress–strain response of reconstituted Petobo soil samples with different fines contents. The analysis focuses on contractive behavior leading to the critical state, pore-pressure buildup, effective stress paths, and normalized residual shear strength within the CSSM framework. Although Artati et al. (2023) examined steady-state liquefaction resistance for Palu silty soils, their work did not investigate residual behavior or post-liquefaction stress-strain evolution.

Therefore, the purpose of this study is to provide the first laboratory-based residual shear strength data for Petobo soil, quantify the influence of fines content under very loose density conditions, and offer mechanistic insight into the 2018 flowslide. These findings provide essential input for back-analysis, numerical modeling, and hazard assessment of liquefaction-induced failures in Palu and similar environments.

METHOD

Material - Location and Samples

The soil samples were collected from Petobo Sub-district, Palu City, one of the areas most severely affected by liquefaction during the 28 September 2018 earthquake. This area experienced large-

scale flow liquefaction extending approximately 2.1 km, resulting in massive ground displacement and the destruction of thousands of houses. The tested soils were taken from a loose sand layer at the ground surface within a residential area affected by flow.

Two types of samples were obtained to represent different fines contents.

1. The low-fines sample (9%), taken from Point A located at a drainage dike (Figure 1a), represents the initiation zone of flow liquefaction.
2. The high-fines sample (26.4%), taken from Point B (Figure 1b), represents the main zone affected by massive ground flow.

A general overview of the affected area and sampling points is shown in Figure 1c.

Figure 1. Sampling locations in Petobo: (a) drainage dike (Location A), (b) area affected by massive ground flow (Location B), (c) overview of the flow liquefaction-affected zone

Soil Characterization

The index properties of the soil were determined through standard ASTM and SNI procedures, including grain size distribution (ASTM D6913 for sieve analysis; ASTM D7928 for hydrometer; SNI 3423:2008), specific gravity (ASTM D854 maximum and minimum index densities (ASTM D4253 and ASTM D4254), Atterberg limits (ASTM D4318), and natural water content (ASTM D2216).

The grain size curves are presented in Figure 2, and the index properties are summarized in Table 1.

Two groups of soils were identified:

1. Low-fines sand (9%), approaching clean sand, obtained from Location A (Figures 1a and 1c).
2. High-fines sand (26.4%), classified as SC according to the Unified Soil Classification
3. System (USCS). However, based on visual observation and mechanical behavior, this soil more closely resembles silty sand. It was obtained from Location B (Figures 1b and 1c**).**

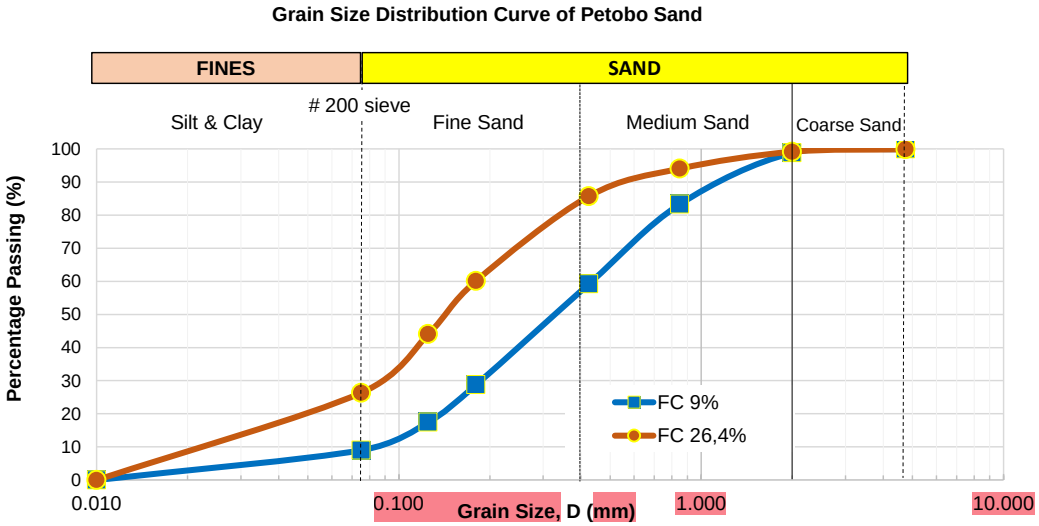

Figure 2. Grain size distribution of soil samples with fines content of 9% and 26.4%.

Table 1. Index properties of Petobo sand samples with fines contents of 9% and 26.4%

Sifat - sifat Indeks	Sampel A	Sampel B
Gs	2,7	2,69
Gravel (%)	0	0
Coarse Sand (%)	1,17	0,09
Medium Sand (%)	39,58	13
Fine Sand (%)	50,25	59
Fines Content	9,01	26
D_{50} (mm)	0,32	0,15
D_{10} (mm)	0,08	0,02
D_{30} (mm)	0,18	0,09
D_{60} (mm)	0,35	0,18
Cc	1,23	2,05
Cu	4,67	8,18
PL (%)	NP	20,65
PI (%)	0	13,65
Soil Classification (USCS)	SP - SM	SC
$\rho_{d\,max}$ (Mgr/cm^3)	1,48	1,60
$\rho_{d\,min}$ (Mgr/cm^3)	1,20	1,22
e_{max}	1,250	1,209
e_{min}	0,821	0,680

Specimen Preparation

Six specimens were prepared in total: three with low fines content (9%) and three with high fines content (26.4%). Each set was tested under initial mean effective stresses (p'_0) of 100, 150, and 200 kPa. The specimens were cylindrical, 38 mm in diameter and 76 mm in height.

All specimens were prepared in a very loose condition (Dr = 11-20%), consistent with the natural looseness of the Petobo sand, to ensure a contractive response and convergence toward the critical state during monotonic loading.

Figure 3. Specimen preparation using the moist tamping (undercompaction) method

p-ISSN: 1410-2331 e-ISSN: 2460-1217

The moist tamping (undercompaction) method (Figure 3) was adopted, as originally proposed by Ladd and widely recommended in recent studies on silty sands[9], [10], [12]. This method was selected because it:

1. enables the preparation of specimens in a very loose state, representative of post-liquefaction conditions,
2. minimizes segregation of fine particles during sample assembly, and
3. is more practical than alternative methods such as air pluviation or slurry deposition.

Consolidated Undrained (CU) Triaxial Test Procedure

Monotonic Consolidated Undrained (CU) triaxial compression tests were conducted in accordance with ASTM D4767 (2011) and SNI 03-2455:1991 (Figure 4). The CU test was selected because it simulates the undrained behavior of saturated soils under axial loading and allows measurement of excess pore water pressure (Δu), deformation, and the effective stress path ($p' - q$).

The testing procedure consisted of the following stages:

1. Saturation stage. The specimens were saturated by applying back pressure until the Skempton parameter (B-value) reached ≥ 0.95. This step was essential to ensure full saturation so that any volume change would be entirely governed by pore water pressure. Ensuring full saturation and consistent test repeatability aligns with the recommended laboratory procedures for obtaining reliable critical-state behavior in triaxial testing [24].
2. Isotropic consolidation stage. Once saturation was achieved, the specimens were isotropically consolidated under initial mean effective stresses (p'_0) of 100, 150, and 200 kPa. These stress levels simulated different in-situ effective stress conditions corresponding to soil depth. This stress range reflects the effective stress conditions of the upper 5-10 m of the Petobo deposit, which correspond to the zone where liquefaction triggering and flow deformation were observed during the 2018 Palu event.
3. Monotonic shearing stage. The specimens were axially loaded under strain-controlled conditions at a constant rate of 0.05 mm/min. The tests were continued until axial strains exceeded 20% to ensure that the soil specimens reached the critical state

Figure 4. Consolidated Undrained (CU) triaxial compression test apparatus

Repeatability and Error Control

Each test condition was performed at least twice to verify repeatability. Differences in peak and residual deviator stresses remained within ±5%, which is within the acceptable tolerance for manually controlled triaxial tests on natural sands as established in classical laboratory guidelines (Head, 1998) and confirmed in more recent studies on silty sands [31].

Average values from the repeated tests were used in analysis, and any test showing deviations beyond this threshold was excluded. The consistent trends confirm that the measured stress-strain response and residual strength are representative and reliable.

Test Data and Graphical Results

The CU tests produced the following curves:

1. stress–strain curves ($q - \varepsilon$),
2. excess pore water pressure development ($\Delta u - \varepsilon$), and
3. effective stress paths ($p' - q$).

Parameter Calculation

1. Deviator stress (q):
$$q = (\sigma'_1{}' - \sigma'_3) = \Delta\sigma \quad (1)$$

representing the mobilized shear stress in the specimen. This parameter quantifies the magnitude of shear resistance or the additional axial load sustained by the soil during undrained shearing.

2. Mean effective stress (p'):

$$p' = \frac{1}{3}(\sigma'_1 + 2\sigma'_3) \quad (2)$$

representing the average effective stress carried by the soil skeleton after accounting for pore water pressure. This parameter was used to construct the effective stress path.

3. Excess pore water pressure (Δu):

representing the pore pressure generated during axial loading. Δu was continuously recorded to illustrate the mechanism of effective stress reduction and to identify the tendency toward contractive or dilative response.

Where σ'_1 is the axial effective stress and σ'_3 is the confining effective stress.

These parameters were computed at each loading increment to capture the evolution of stress and pore-pressure during undrained shearing

Justification for Using Monotonic CU Triaxial Tests

Although liquefaction in the field is a cyclic phenomenon, cyclic triaxial tests are often difficult to control at large strains because very loose silty sands rapidly lose stiffness and may reach instability before the residual condition is achieved. Monotonic undrained triaxial tests overcome this limitation by allowing continuous shearing to large strains, enabling direct measurement of residual or steady-state shear strength under a controlled stress path. This approach has long been used for post-liquefaction characterization and is still supported by recent studies showing that monotonic and cyclic responses can be interpreted consistently within modern critical-state or equivalent-state frameworks [10][23]. Updated laboratory recommendations further emphasize the suitability of controlled monotonic shearing for obtaining reliable critical-state parameters in cohesionless soils [24]. Based on these advantages, the monotonic Consolidated Undrained (CU) triaxial test was selected to evaluate the post-liquefaction residual behavior of Petobo silty sand within the critical-state framework.

Data Analysis

The results were interpreted within the framework of Critical State Soil Mechanics (CSSM), which provides a conceptual basis to describe the transition of saturated sand from contractive to steady-state or critical conditions under undrained loading. This framework was used to evaluate the evolution of deviator stress (q), mean effective stress p' and excess pore water pressure (Δu) until a nearly constant stress ratio was reached, representing the critical or residual state. Recent recommendations for triaxial evaluation of critical-state behavior in cohesionless soils also emphasize interpreting stress paths consistently with the critical state locus [24]. The influence of fines content on this stress-strain evolution and the resulting residual strength was then assessed to understand the post-liquefaction behavior of Petobo silty sand

RESULTS AND DISCUSSION

The results of the CU triaxial tests on Petobo sand are summarized in Table 2, which presents the maximum deviator stress (q_{max}), maximum excess pore water pressure (Δu_{max}), and residual strength for the two fines contents (9% and 26.4%) under three levels of confining stress, or initial mean effective stress (p'_0) within the CSSM framework. The stress–strain ($q-\varepsilon$), pore-pressure-strain ($\Delta u-\varepsilon$), and and effective stress path ($p'-q$) relationships are shown in Figures 5-7 to illustrate the soil response under undrained loading.

Table 2. Summary of CU triaxial test results

Fine Content (FC %)	p'_0 (kPa)	q_{max} (kPa)	Δu (kPa)	$q_{residual}$ (kPa)	$q_{residual}/p'_0$
9	100	106.13	62.10	89.47	0.89
9	150	134.36	95.40	126.91	0.85
9	200	186.62	123.20	177.73	0.89
26.4	100	104.75	62.35	93.54	0.94
26.4	150	130.21	102.00	118.30	0.79
26.4	200	190.04	127.60	178.12	0.89

SINERGI Vol. xx, No. x, February 20xx: xxx-xxx
http://publikasi.mercubuana.ac.id/index.php/sinergi
http://doi.org/10.22441/sinergi.xxxx.x.xxx

Stress-Strain Behavior $(q-\varepsilon)$

The stress–strain curves (Figure 5) show a characteristic response of very loose silty sand, marked by a rapid increase in deviator stress at small strains, followed by a broad plateau extending to large strains (ε > 10%). The curves do not exhibit pronounced strain softening; instead, the deviator stress gradually approaches a nearly constant level, indicating that the specimens attained a stable residual or critical state without significant post-peak reduction in strength.

The peak deviator stress (q_{max}) increases systematically with the initial mean effective stress (p'_0), consistent with typical behavior of loose granular materials under undrained loading. Differences between the 9% and 26.4% fines content groups are relatively small, generally within 1-5% for q_{max}, reflecting that, at very loose densities (Dr = 11% for FC 9% and Dr = 20% for FC 26.4%), the peak shear response is governed predominantly by the sand skeleton. The influence of fines becomes more apparent in pore-pressure generation (Δu) and in the curvature of the effective stress paths rather than in the peak deviator stress itself.

Although loose clean sands typically exhibit a sharp drop in deviator stress after the peak, loose silty sands such as the Petobo material tend to show more moderate softening. The presence of non-plastic fines and the angularity of volcanic grains reduce the abruptness of post-peak strain softening, resulting in a smaller difference between q_{max} and q_{res}. Despite this, all specimens clearly reach the critical state, mobilizing low normalized residual strength ratios (q_{res}/p'_0 = 0.79-0.94), which remain indicative of high flow-liquefaction susceptibility.

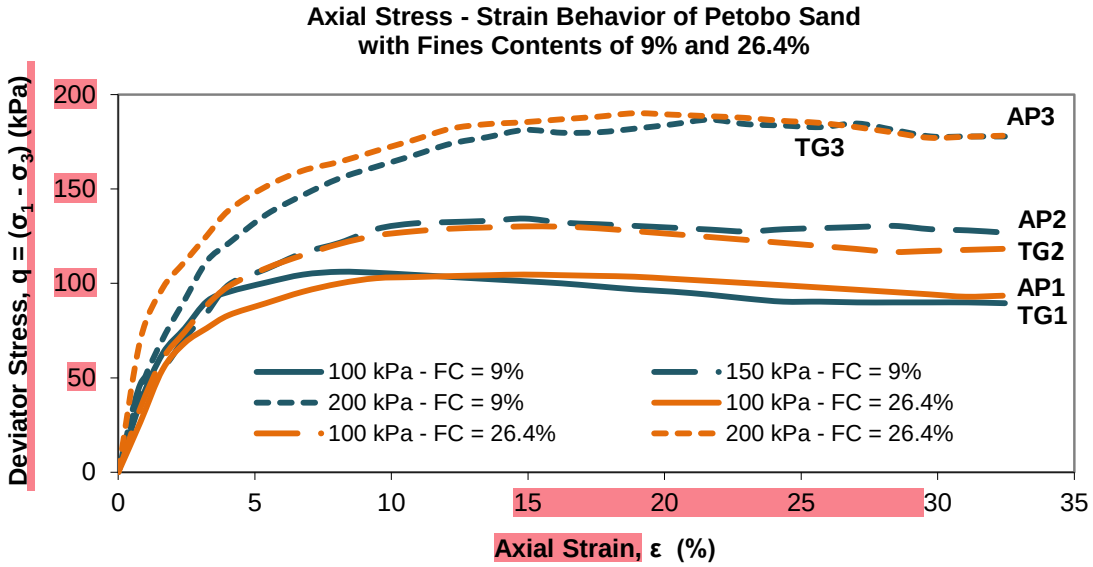

Figure 5. Stress–strain $(q-\varepsilon)$ behavior of Petobo sand at fines contents of 9% and 26.4% under initial mean effective stresses of 100, 150, and 200 kPa.

Excess Pore Water Pressure Development $(\Delta u-\varepsilon)$

The $\Delta u-\varepsilon$ curves (Figure 6) show a rapid increase in excess pore water pressure at small strains (<10%) for all specimens, indicating strong contractive behavior typical of very loose sands. Both fines-content groups (FC = 9% and FC = 26.4%) reached similar maximum excess pore-pressures Δu_{max}, demonstrating that at very low relative densities (Dr = 11-20%), the predominant factor governing pore-pressure buildup is the loose, compressible sand skeleton rather than fines content alone.

Specimens with 26.4% fines generated slightly higher Δu at intermediate strains, but the overall difference in Δu_{max} between the two fines contents remained modest (generally within 5%). This suggests that, within the tested density range, fines influence the rate and shape of pore-pressure accumulation more strongly than the absolute magnitude Δu_{max}

These observations are consistent with recent experimental studies on loose silty sands, which report that non-plastic fines modify soil microstructure and compressibility but do not necessarily produce large increases in Δu_{max} unless there is a substantial density contrast between specimens [10][9]. Additional hydraulic factors, such as partial saturation, pore fluid compressibility, and strain rate, have also been shown to influence the intensity and timing of pore-pressure generation, particularly at small strains [32]. The minor differences observed in Δu between the two fines-content groups are therefore attributable to a combination of microstructural and hydraulic effects.

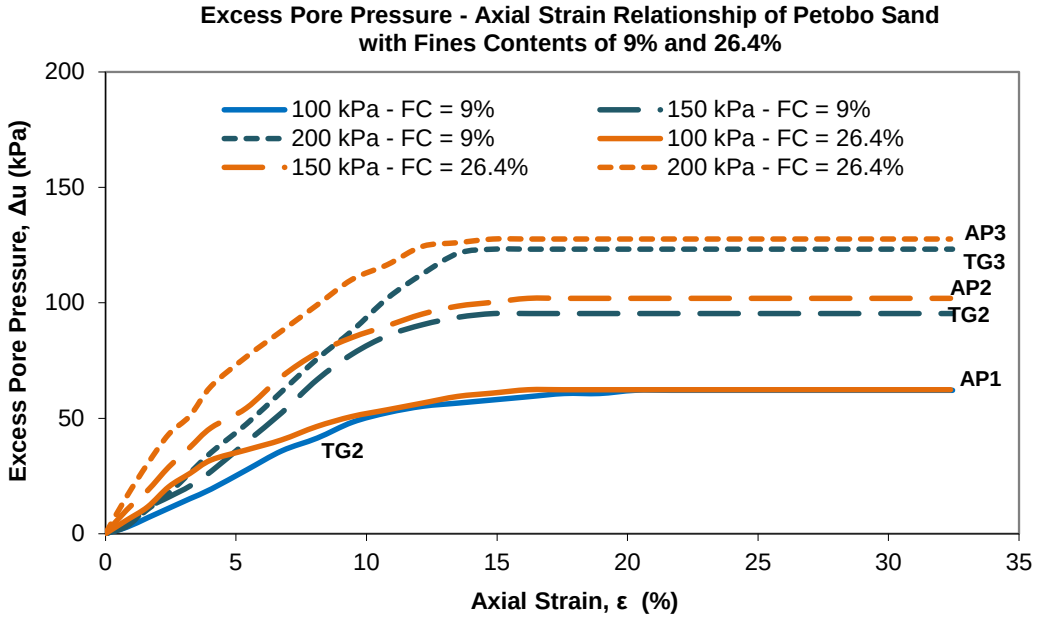

Figure 6. Excess pore water pressure-strain $(\Delta u - \varepsilon)$ curves of Petobo sand at different fines contents and initial mean effective stresses

Critical State Line (CSL)

The Critical State Line (CSL) defines the condition at which soil continues to deform at constant shear stress, effective mean stress, and volume. Within the framework of Critical State Soil Mechanics (CSSM), the slope of the line in $p' - q$ space ($M = q/p'$) represents the critical-state stress ratio and provides a quantitative index of the soil's steady-state shear strength.

In this study, the CSL was derived from monotonic CU triaxial tests on reconstituted Petobo silty sand. The steady-state portion of each effective stress path was identified at large strains (=15-20%), where both deviator stress (q) and mean effective stress (p') approached nearly constant values. The corresponding stress ratio $M = q/p'$ was calculated to determine the critical-state stress ratio for each specimen.

The computed M-values were consistent within each fines-content group, averaging about 1.312 for FC = 9% and 1.355 for FC = 26.4%. Although recent studies on silty and volcanic derived sands do not report explicit numerical M-values for specific fines contents, they consistently show that fines influence contractive tendency, pore-pressure generation, and the curvature of the effective stress path rather than producing major shifts in the CSL slope itself [16], [23], [26], [27]. This behavior aligns with the present results, where both fines levels converged toward similar critical-state stress ratios despite noticeable differences in early-stage contractive behavior and residual strength.

The quantitative M-values used to construct the CSL are summarized in Table 3, and the corresponding effective stress paths are presented in Figure 7.

Table 3. Summary of Critical-State Stress Ratios

Spec	FC (%)	p'_0 (kPa)	$M = \frac{q}{p'}$	Behavior
TG1	9	100	1.321	Contractive
TG2	9	150	1.310	Contractive
TG3	9	200	1.306	Contractive
Average (FC = 9%)			**1.312**	
AP1	26.4	100	1.359	Contractive
AP2	26.4	150	1.353	Contractive
AP3	26.4	200	1.352	Contractive
Average (FC = 26.4%)			**1.355**	

Effective Stress Path ($p'-q$)

The effective stress paths (Figure 7) consistently moved downward to the left, reflecting the progressive reduction in mean effective stress (p') associated with contractive behavior under undrained loading. The addition of fine particles significantly influenced this contractive response. Specimens with higher fines content (FC = 26.4%) shifted more rapidly toward the lower-left region of the $p'-q$ plane compared to those with lower fines content (FC = 9%). This tendency indicates greater excess pore water pressure (Δu) generation at small strains (< 10%). This trend is consistent with previous findings that non-plastic fines intensify contractive response and accelerate [9][10].

At larger strains, however, the two soils diverged markedly. The high-fines specimens reached slightly higher normalized residual strength ratios (q_{res}/p'_0 = 0.79-0.94) compared with the low-fines specimens (q_{res}/p'_0 = 0.85-0.89) (Table 2). This suggests that although the 26.4% fines samples were initially more contractive, they ultimately stabilized at comparable or somewhat stronger residual conditions. This behavior can be attributed to fine particles improving packing density and increasing the number of interparticle contacts [12].

Therefore, the influence of fines on liquefaction response is nonlinear: higher fines content enhances contractive tendency during initiation but can modestly improve stabilization during the post-liquefaction phase. These results demonstrate the need to distinguish between liquefaction initiation susceptibility and post-liquefaction stability within the critical-state framework.

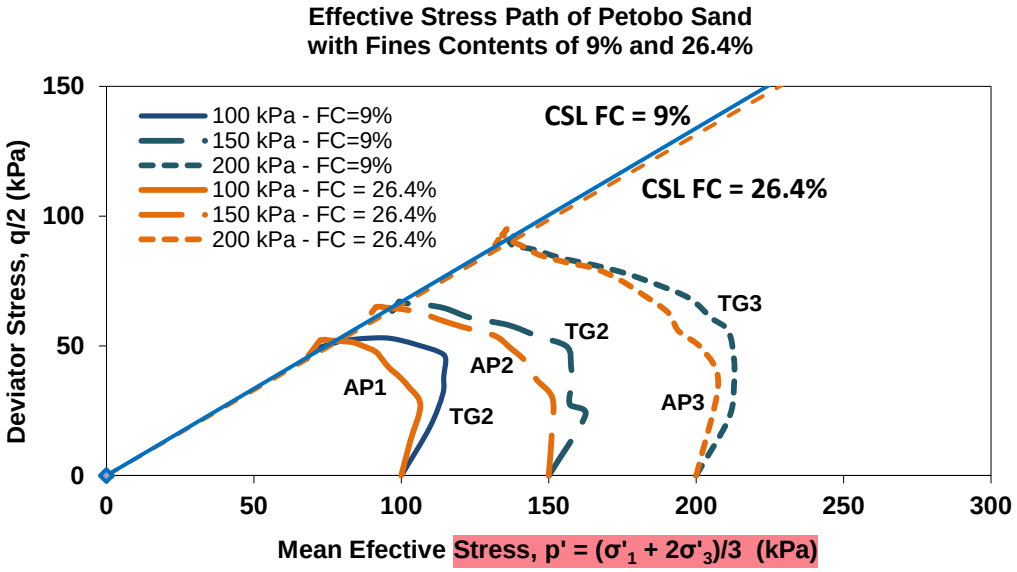

Figure 7. Effective stress paths ($p'-q$) of Petobo sand at different fines contents and initial mean effective stresses

Empirical Relationship and Validation with CSSM Framework

The CU triaxial results show that the normalized residual strength ratio (q_{res}/p'_0) exhibits only minor variation between the two fines-content groups. For FC = 9%, the ratio ranges from 0.85-0.89, while for FC = 26.4% it ranges from 0.79-0.94, giving nearly identical averages of approximately 0.88 for both soils. This indicates that, at very loose initial densities (Dr = 11-20%),

fines content does not produce a systematic increase in residual strength. Instead, the post-liquefaction resistance is governed primarily by the loose fabric of the sand skeleton and the effective stress level at the onset of steady-state shearing.

Although fines do not significantly alter the absolute value of (q_{res}/p'_0), a weak empirical trend can still be represented by a simple best-fit regression across all six specimens:

$$q_{res}/p'_o = -0.00019 \cdot FC + 0.878$$

The essentially zero slope and very low R^2 confirm that fines content is not a meaningful predictor of residual strength under the very loose density conditions tested. Instead, fines primarily influence the shape of the effective stress path and the rate of pore-pressure generation, rather than the final post-liquefaction resistance.

Table 3 summarizes the critical-state stress ratio ($M = q/p'$) obtained from the large-strain portion of the effective stress paths. The measured M-values range from 1.306 to 1.359, which lies within the typical range reported for loose silty sands and volcanic-derived granular materials in recent CSSM studies. This indicates that both fines-content levels converge toward a similar critical-state condition, reinforcing the interpretation that fines modify early-stage contractive behavior but do not significantly alter the ultimate steady-state shear strength.

Overall, the empirical trend and critical-state validation indicate that fines content in loose Petobo sand acts mainly as a modifier of the contractive response and effective stress path curvature, rather than as a direct determinant of residual strength. This distinction is important for constitutive modeling, where fines-dependent parameters should focus on initiation and pore-pressure buildup rather than residual strength alone.

Effect of Initial Mean Effective Stress (p'_0)

Increasing the initial mean effective stress (p'_0) from 100 to 200 kPa increased the maximum deviator stress $(q_{\max})$ for both fines-content groups, indicating that specimens consolidated under higher confining pressures mobilized greater shear resistance. However, the normalized residual strength ratio (q_{res}/p'_0) did not increase proportionally with p'_0. This trend is consistent with Critical State Soil Mechanics (CSSM), which predicts that specimens sheared from higher initial effective stresses approach the critical state along paths that yield higher absolute residual strength but similar or lower normalized strength ratios

The measured data confirm this behavior. For FC = 9%, residual strength increased from q_{res} = 89.47 kPa at p'_0 = 100 kPa to q_{res} = 177.73 kPa at p'_0 = 200 kPa, yet the normalized ratio remained nearly constant (q_{res}/p'_0 = 0.89) with a slight dip at intermediate p'_0 = 150 kPa (0.85). A similar pattern was observed for FC = 26.4%, where q_{res} increased from 93.54 kPa to 178.12 kPa,

These results demonstrate the characteristic stress-ratio dilution effect, where increases in p'_0 elevate the absolute shear capacity but do not produce proportional increases in normalized residual strength. This behavior is consistent with recent CSSM-based studies on saturated silty sands and volcanic-derived materials, which report comparable reductions or plateaus in normalized strength at higher consolidation stresses.

The interaction between fines content and initial stress is also evident. Non-plastic fines enhance packing density and improve shear resistance at large strains, but their influence on normalized residual strength is moderated by the initial effective stress. In contrast, soils containing plastic or highly compressible fines have been shown to experience larger reductions in residual strength under similar conditions, highlighting the importance of fines characteristics.

This laboratory trend aligns with field observations in Petobo. Deeper layers subjected to higher overburden stresses (higher p'_0) likely mobilized lower residual strength ratios, while shallower loose layers with lower p'_0 experienced greater displacement and more extensive flow deformation during the 2018 event. Thus, the experimental results provide a realistic representation of the stress-controlled spatial variability observed in the field.

Implications for Post-Liquefaction Stability and Relevance to the 2018 Palu Flowslide

The laboratory results show that both low-fines and high-fines specimens of Petobo sand exhibit low normalized residual strength (q_{res}/p'_0 = 0.79-0.94), confirming their high susceptibility to flow-type deformation once liquefaction is triggered. Although specimens with 26.4% fines mobilized slightly higher residual strength values, the differences between the two fines levels are small, indicating that fines have only a limited influence on steady-state shear resistance under very loose initial densities. These trends suggest that fines mainly affect early-stage contractive behavior and pore-pressure generation, while the final post-

p-ISSN: 1410-2331 e-ISSN: 2460-1217

liquefaction resistance is governed predominantly by the loose sand fabric and the effective stress level at the onset of steady state.

The relevance of these findings becomes clearer when viewed in the context of previous investigations of the 2018 Palu flowslides. Earlier field assessments [29], [33] reported that the large runout observed in Petobo was driven by a substantial loss of shear strength after liquefaction, yet no laboratory-based residual strength values for the local soils were available. Post-earthquake reconnaissance surveys [30] also documented extensive flow deformation but highlighted the absence of experimental strength measurements needed to support quantitative back-analyses. The residual strength ratios obtained in this study provide the first experimental reference for Petobo silty sand, helping explain why the deposits were capable of undergoing long-runout flow deformation during the earthquake and offering essential parameters for future modeling and hazard assessment of liquefaction-induced flow failures in Palu and similar environments.

These findings reinforce that Petobo-type deposits, when liquefied, are mechanically capable of sustaining long-distance mobility, highlighting the need to incorporate residual strength variability into future land-use planning and reconstruction policies in Palu

Research Limitations

This study was conducted using six reconstituted specimens tested under monotonic consolidated undrained (CU) triaxial loading. Although effective for identifying post-liquefaction residual behavior within the CSSM framework, monotonic loading does not capture the cyclic stress accumulation mechanisms that trigger liquefaction during real earthquakes. The use of remolded samples prepared by moist tamping also limits the representation of natural depositional fabric and stratigraphic variability in the in-situ Petobo profile.

The tests were performed on very loose silty sands, and achieving stable full saturation required extended preparation, which may introduce minor uncertainties in saturation uniformity. Given these limitations, the results should be interpreted as controlled laboratory observations intended to characterize fundamental trends in stress–strain response, pore-pressure generation, and residual strength under undrained monotonic loading.

Future research should incorporate cyclic triaxial or simple-shear tests, alternative reconstitution procedures, and larger specimen sets to improve generalization. Numerical back-analyses of the 2018 Petobo flowslide using the residual strengths obtained here are also recommended to strengthen the connection between laboratory behavior and field-scale deformation.

CONCLUSION

This study demonstrates that loose Petobo sand is highly susceptible to liquefaction, as indicated by rapid excess pore-water pressure buildup and effective stress paths converging toward the critical state. Although fines content affects early-stage contractive behavior and pore-pressure generation, its influence on the final post-liquefaction resistance is minimal. The normalized residual strength ratios for both fines levels fall within a narrow range (q_{res}/p'_0 = 0.79-0.94), indicating that the ultimate shear resistance is governed primarily by the very loose sand fabric and the effective stress level at steady state rather than by fines content.

These findings help reconcile differences reported in previous studies that identified fines-dependent variations in steady-state resistance. The results demonstrate that under very loose initial densities, the influence of fines on residual strength diminishes significantly, and the post-liquefaction response becomes dominated by fabric collapse and rapid loss of effective stress. This clarification enhances understanding of the flow-failure mechanisms observed during the 2018 Petobo event and provides a more clearly defined empirical basis within the CSSM framework.

As a preliminary investigation, this work is limited by the small number of specimens, the use of reconstituted samples, and the absence of cyclic loading. Future studies should incorporate cyclic and stress-controlled triaxial tests, evaluation of equivalent granular state parameters, and coupled numerical modeling to develop a more comprehensive representation of liquefaction triggering and post-liquefaction stability in silty sand deposits of Central Sulawesi.

This study fills a critical data gap for Palu and provides benchmark residual strength values that can be directly used in numerical back-analysis and disaster mitigation planning

ACKNOWLEDGMENT

The authors would like to thank their colleagues at the Soil Mechanics Laboratory of Parahyangan Catholic University and Universitas Mercu Buana for their technical support and valuable input during the course of this research and the preparation of this article.

REFERENCES

[1] A. P. Gallant *et al.*, "The Sibalaya flowslide initiated by the 28 September 2018 MW 7.5 Palu-Donggala, Indonesia earthquake," *Landslides*, vol. 17, no. 8, pp. 1925–1934, 2020.
[2] A. Jalil, T. F. Fathani, I. Satyarno, and W. Wilopo, "Liquefaction in Palu: the cause of massive mudflows," *Geoenvironmental Disasters*, vol. 8, no. 1, 2021.
[3] A. Rahayu, I. Uno, N. Hidayat, A. Dwijaka, and M. Yusuf, "Potential of Liquifaction at Nasanapura Hospital Petobo Village Palu City," *IOP Conf. Ser. Earth Environ. Sci.*, vol. 1075, no. 1, 2022.
[4] M. Simatupang, R. S. Edwin, and Sulha, "Liquefaction severity assessment for the Anutapura Medical Center Area of Palu-Indonesia," *IOP Conf. Ser. Earth Environ. Sci.*, vol. 1195, no. 1, 2023.
[5] L. E. Widodo, S. H. Prassetyo, G. M. Simangunsong, and I. Iskandar, "Role of the confined aquifer in the mechanism of soil liquefaction due to the 7.5 Mw earthquake in Palu (Indonesia) on 28 September 2018," *Hydrogeol. J.*, vol. 30, no. 6, pp. 1877–1898, 2022.
[6] T. C. Upomo, M. Chang, R. Kusumawardani, G. A. Prayitno, C.-P. Kuo, and U. Nugroho, "Assessment of Petobo Flowslide Induced by Soil Liquefaction during 2018 Palu–Donggala Indonesian Earthquake," *Sustainability*, vol. 15, no. 6, p. 5371, Mar. 2023.
[7] V. Jayakrishnan, K. S. Beena, and C. B. Blayil, "Studying the Impact of Continuous and Multiple Earthquake Ground Motions on Pore Pressure in Saturated Sandy Deposits," *Geotech. Geol. Eng.*, vol. 42, no. 6, pp. 5375–5387, Aug. 2024.
[8] K. O. Cetin and H. T. Bilge, "Recent advances in seismic soil liquefaction engineering," *Evol. Geotech - 25 Years Innov.*, no. 2001, pp. 18–42, 2022.
[9] L. Jradi, B. S. El Dine, J. C. Dupla, and J. Canou, "Influence of low fines content on the liquefaction resistance of sands," *Eur. J. Environ. Civ. Eng.*, vol. 26, no. 12, pp. 6012–6031, 2022.
[10] A. Ghorbani, A. Eslami, and M. Nezhad Moghadam, "Effect of non-plastic silt on liquefaction susceptibility of marine sand by transparent laminar shear box in shaking table," *Int. J. Geotech. Eng.*, vol. 00, no. 00, pp. 1–13, 2020.
[11] H. Artati, W. Pawirodikromo, P. Rahardjo, and L. Makrup, "Effect of Fines Content on Liquefaction Resistance During Steady-State Conditions," *Int. J. GEOMATE*, vol. 25, no. 109, pp. 18–28, 2023.
[12] S. Gobbi, P. Reiffsteck, L. Lenti, M. P. S. d'Avila, and J. F. Semblat, "Liquefaction triggering in silty sands: effects of non-plastic fines and mixture-packing conditions," *Acta Geotech.*, vol. 17, no. 2, pp. 391–410, 2022.
[13] M. Goudarzy, D. Sarkar, and T. Wichtmann, "Influence of plastic fines content on the liquefaction susceptibility of sands: cyclic loading," *Acta Geotech.*, vol. 17, no. 11, pp. 4977–4988, 2022.
[14] C. P. Polito, J. R. Martin, and E. L. D. Sibley, "The Effect of Non-Plastic Fines Content on Pore Pressure Generation Rates in Cyclic Triaxial and Cyclic Direct Simple Shear Tests," *Eng*, vol. 5, no. 4, pp. 2410–2427, 2024.
[15] H. Saeed, Z. Nalbantoglu, and E. Uygar, "Liquefaction susceptibility of beach sand containing plastic fines," *Mar. Georesources Geotechnol.*, vol. 41, no. 1, pp. 1–13, 2023.
[16] G. Tomasello and D. D. Porcino, "Energy-Based Pore Pressure Generation Models in Silty Sands under Earthquake Loading," *Geosci.*, vol. 14, no. 6, 2024.
[17] X. Wei, J. Yang, and Z.-X. Yang, "Characterizing the Liquefaction Potential and Pore Pressure Generation of Silty Sands through the Energy-Based Approach in the Framework of Critical State Soil Mechanics," *J. Geotech. Geoenvironmental Eng.*, vol. 150, no. 10, Oct. 2024.
[18] S. Ćorluka, D. Rakić, N. Živanović, K. Djoković, and T. Đurić, "A Correlation Relating the Residual Strength Parameters to the Proportions of Clay Fractions and Plasticity Characteristics of Overburden Sediments from the Open-Pit Mine Drmno," *Appl. Sci.*, vol. 14, no. 22, 2024.
[19] Z. Li, S. Escoffier, and P. Audrain, "Study on the effects of a low amount of non-plastic fines on soil liquefaction by dynamic centrifuge modeling," *Soil Dyn. Earthq. Eng.*, vol. 195, p. 109400, Aug. 2025.
[20] G. Chen *et al.*, "New paradigm for sand liquefaction under cyclic loadings," *Eng. Geol.*, vol. 351, p. 108041, May 2025.
[21] M.-A. Abdul-Khader and S. Jeong, "Behavior of Weathered Soil under Combined Undrained Cyclic-Monotonic Loading," *Int. J. Geomech.*, vol. 21, no. 4, Apr. 2021.
[22] I. D. Gates and M. Ghayoomi, "Residual Strength of Liquefied Soil: The Effect of Induced Partial Saturation," *Geotech. Test. J.*, vol. 45, no. 4, pp. 855–876, Jul. 2022.
[23] A. Papadopoulou and T. Tika, "Monotonic and cyclic behaviour of sand-silt mixtures through the equivalent state parameter," in *E3S Web of Conferences*, 2024, pp. 544,

14014.
[24] A. V. da Fonseca, D. Cordeiro, and F. Molina-Gómez, “Recommended Procedures to Assess Critical State Locus from Triaxial Tests in Cohesionless Remoulded Samples,” *Geotechnics*, vol. 1, no. 1, pp. 95–127, 2021.
[25] Y. Wu, M. Hyodo, and J. Cui, “On the critical state characteristics of methane hydrate-bearing sediments,” *Mar. Pet. Geol.*, vol. 116, no. March, p. 104342, 2020.
[26] H. B. K. Nguyen, M. M. Rahman, and A. B. Fourie, “How particle shape affects the critical state, triggering of instability and dilatancy of granular materials - Results from a DEM study,” *Geotechnique*, vol. 71, no. 9, pp. 749–764, 2021.
[27] G. Wanli and C. Zhengyin, “Study on the critical state of a unique silty sand,” *Granul. Matter*, vol. 24, no. 1, pp. 1–8, 2022.
[28] Z. Fan, R. Cudmani, S. Chrisopoulos, X. Xiong, M. Sun, and Y. Yuan, “Experimental study on the reliquefaction behavior of saturated sand deposits under distinct loading frequencies,” *Soil Dyn. Earthq. Eng.*, vol. 190, p. 109114, Mar. 2025.
[29] H. B. Mason *et al.*, “East Palu Valley Flowslides Induced by the 2018 MW 7.5 Palu-Donggala Earthquake.,” *Geomorphology*, vol. East Palu, 2020.
[30] J. Montgomery, J. Wartman, A. N. Reed, A. P. Gallant, D. Hutabarat, and H. B. Mason, “Field reconnaissance data from GEER investigation of the 2018 M W 7 . 5 Palu-Donggala earthquake,” *Data Br.*, vol. 34, p. 106742, 2021.
[31] Y. Yang, B. Yang, C. Su, and J. Ma, “Application of Residual Shear Strength Predicted by Artificial Neural Network Model for Evaluating Liquefaction-Induced Lateral Spreading,” *Adv. Civ. Eng.*, vol. 2020, 2020.
[32] M. Cueva, X. Kang, S. Wang, E. Soranzo, and W. Wu, “Unveiling the role of saturation and displacement rate in the transition from slow movement to catastrophic failure in landslides,” *Eng. Geol.*, vol. 352, no. April, p. 108042, 2025.
[33] A. Jalil, T. F. Fathani, I. Satyarno, and W. Wilopo, “A study on the liquefaction potential in banda aceh city after the 2004 sumatera earthquake,” *Int. J. GEOMATE*, vol. 18, no. 65, pp. 147–155, 2020.